Author's Accepted Manuscript

An optimization model for assessment of membrane-based post-combustion gas upcycling into hydrogen or syngas

Gabriel Zarca, Ane Urtiaga, Lorenz T. Biegler, Inmaculada Ortiz

www.elsevier.com/locate/memsci

PII: S0376-7388(18)30094-2
DOI: https://doi.org/10.1016/j.memsci.2018.05.038
Reference: MEMSCI16178

To appear in: *Journal of Membrane Science*

Received date: 11 January 2018
Revised date: 9 May 2018
Accepted date: 19 May 2018

Cite this article as: Gabriel Zarca, Ane Urtiaga, Lorenz T. Biegler and Inmaculada Ortiz, An optimization model for assessment of membrane-based post-combustion gas upcycling into hydrogen or syngas, *Journal of Membrane Science,* https://doi.org/10.1016/j.memsci.2018.05.038

This is a PDF file of an unedited manuscript that has been accepted for publication. As a service to our customers we are providing this early version of the manuscript. The manuscript will undergo copyediting, typesetting, and review of the resulting galley proof before it is published in its final citable form. Please note that during the production process errors may be discovered which could affect the content, and all legal disclaimers that apply to the journal pertain.

© 2018. This manuscript version is made available under the CC-BY-NC-ND 4.0 license http://creativecommons.org/licenses/by-nc-nd/4.0/

ACCEPTED MANUSCRIPT

An optimization model for assessment of membrane-based post-combustion gas upcycling into hydrogen or syngas

Gabriel Zarca[a,*], Ane Urtiaga[a], Lorenz T. Biegler[b], Inmaculada Ortiz[a]

[a]Department of Chemical and Biomolecular Engineering, Universidad de Cantabria, Av. Los Castros 46, Santander 39005, Spain.

[b]Department of Chemical Engineering, Carnegie-Mellon University, 5000 Forbes Avenue, Pittsburgh, Pennsylvania 15213-3890, United States

*Corresponding author e-mail address: zarcag@unican.es

Accepted manuscript

Abstract

In this work, we present an optimization model and techno-economic analysis aimed at assessing the viability of employing membrane technology to recover value-added compounds from post-combustion gases of the process industry. In particular, the tail gas generated in carbon black manufacturing process is targeted. The content of hydrogen (H_2) and carbon monoxide (CO) in this waste gas stream is relatively high, thus the possibility of increasing the sustainability of the process by recovering either H_2 or both compounds simultaneously (syngas) is addressed. A comparison is performed between the optimal process designs for each recovery scenario based on the separation characteristics provided by state-of-the-art and prospective membrane materials. To that end, a two-stage membrane separation process using hollow-fiber membranes is implemented in the General Algebraic Modeling System (GAMS) as a nonlinear programming model (NLP). The optimal process design for each recovery scenario is found determining the feed pressure, membrane area, power consumption and composition of all process streams that meet the specified H_2 recovery and

ACCEPTED MANUSCRIPT

product purity targets at the minimum net present value cost. Results indicate that membrane technology can drive the recovery of significant amounts of H_2 from this unconventional source using the separation potential of current polymeric membranes. Moreover, novel ionic liquid-based membranes may be seen as promising candidates providing the required separation properties to obtain a syngas-rich product stream at a lower cost. In this way, the recovery of value-added products is intensified and the carbon dioxide emissions related to the conventional thermal treatment of the tail gas are partially mitigated, thus also reducing the environmental impact of carbon black manufacturing process.

Keywords

Carbon monoxide, gas separation, hydrogen, membrane technology, process optimization, sensitivity analysis.

Introduction

In a global context of natural resource scarcity and tighter environmental policies, the opportunity has arisen to shift from a linear model of production to circular economy business models that extract value from waste resources. In this new scenario, particular efforts need to be placed on minimizing environmental impacts as well as increasing the efficiency of resource use while creating new employment and business growth [1]. Here, we focus our attention on the abundant and relatively inexpensive flue gases generated after incomplete combustion in some industrial processes. For instance, coke oven gas (COG) containing 39-65% hydrogen (H_2) is produced at a rate of 280-450 m^3 per ton of coal in coke oven batteries [2,3], whereas in the carbon black manufacturing, the production of tail gas containing significant amounts of H_2 and carbon monoxide (CO) -up to 20% and 18% (on dry basis), respectively- is approximately 10,000 m^3 per ton of carbon black [2]. In the current context of increasing world population, intensive agriculture systems and fuel consumption, H_2 has a growing demand for two of its primary uses, i.e., ammonia synthesis and oil refineries, which can be further increased by the

Accepted manuscript

ACCEPTED MANUSCRIPT

development of future energy systems based on the hydrogen economy [4,5]. Although the use of H_2 as energy carrier would require ultra-high purity supply, other applications can afford less pure feedstocks, e.g., hydrodesulphurization and hydrocracking [6]. Moreover, syngas mixtures can be employed in the production of a large variety of chemicals as well as liquid hydrocarbons. Therefore, the selective recovery of H_2 or syngas from the waste gas streams of the abovementioned processes can be seen as a promising opportunity in the interest of increasing sustainable production.

To that end, the availability of enabling technologies will play an important role driving the successful development of circular economy models. In this sense, membrane gas separations are cost-effective advanced separation processes [7] that are growing in importance as a competitive technology to replace conventional energy intensive heat-driven processes in small and medium scale applications [8], particularly when high product purity is not required. However, despite the large amount of research conducted in order to enhance both gas permeability and selectivity of membrane materials [9], their gas separation performance has not significantly evolved over the last decade [10]. This fact is evidenced by the minor shifts observed in the Robeson's upper bound relationship for many gas pairs [11], demonstrating that membrane technology has reached a high level of maturity.

Besides the development of novel membrane materials with improved separation efficiencies, process design becomes a critical issue affecting the economics of membrane-based separation processes. It becomes evident that the use of single-stage membrane processes compromises the separation performance due to the trade-off that exists between product purity and recovery, and consequently, the required final specifications may not be met in common membrane applications [12]. This has led to intensive research on solving optimization problems to find optimal membrane configurations and operating variables. In this sense, available literature studies mainly focus on two different strategies: i) the evaluation of the separation performance of single-stage and multi-stage configurations that

Accepted manuscript

ACCEPTED MANUSCRIPT

are selected based on previous knowledge and heuristics [12,13]; and ii) the simultaneous optimization of operating regimes and multi-stage process layout [14-22]. These complex optimization problems are most usually formulated using mixed-integer nonlinear programming (MINLP), with integer decision variables representing process units and connections between them, although genetic algorithms have also been implemented for this purpose [13,23,24]. On the other hand, nonlinear programming (NLP) is mainly used to optimize operating conditions, and less often for superstructures that embed a limited number of candidate configurations [16].

In this manner, computer aided process engineering has been successfully applied to the design of membrane separation processes. These include the most important membrane industrial applications, e.g., production of nitrogen or oxygen enriched air, natural gas purification and hydrogen recovery from synthesis gas and refinery streams, as well as other membrane applications that are currently under development and research such as carbon dioxide capture, enhanced oil recovery and biogas upgrading. These optimization problems are solved by minimizing either energy consumption and membrane area or some economic expression that takes into consideration those specifications to calculate the gas processing costs of the membrane-based separation process. Moreover, these studies often consider binary mixtures, except for a few cases that deal with multicomponent gas streams [19-22].

Here, different strategies directed towards increasing process sustainability are envisaged and optimized for the selective membrane-based recovery of value-added compounds from tail gases generated in carbon black manufacturing process. The separation of either H_2 or syngas from this unconventional resource poses a challenge due to the presence of significant amounts of the inert component N_2. Since different state-of-the-art and prospective membrane materials are considered, results obtained in this work can also serve as guidance for future research in membrane development.

Accepted manuscript

ACCEPTED MANUSCRIPT

Methodology

Reference flue gas and membrane materials

The flue gas data from a carbon black manufacturing plant are selected as case study in this work. Carbon black is produced by pyrolysis of heavy aromatic oils in a reducing atmosphere and subsequent quenching with water. Because of the low oxygen-content and high temperatures in the reactor, the resulting tail gas is mainly composed of water vapor (30-50%), nitrogen (30-50%), hydrogen (7-14%), carbon monoxide (6-12%) and carbon dioxide (1-5%), as well as traces of sulphur and nitrogen compounds [25]. In the current study, the quenched flue gas is ideally treated as multicomponent mixture characterized by the parameters collected in Table 1, where the following assumptions hold: i) the presence of trace compounds is neglected; and ii) moisture is condensed in a first recovery step. This water vapor condensation stage pursues two targets: the removal of some of the acid and basic trace compounds that may affect the membrane performance under real conditions (e.g., ammonia, hydrogen sulfide) and enhancing process intensification by recovering and reusing this process water, which is highly desirable given that carbon black manufacturing is very water-intensive. Although this work considers the complete removal of water from the flue gas, there is the possibility that water, if present, condensates at temperatures below the dew point of the gas mixture. Condensed water supposes an additional resistance to mass transfer that will reduce the separation performance. Moreover, water can induce plasticization effects that modify the membrane structure permanently, which will also reduce the membrane performance [26].

Accepted manuscript

Table 1. Case study flue gas parameters.

Case study parameters	Value	Unit
Flowrate, F_0	100	kmol/h
Pressure, p_0	1.01	bar
Temperature, T_0	303	K
Composition:		
N_2	62	mol%
H_2	18	mol%
CO	16	mol%

ACCEPTED MANUSCRIPT

CO_2	4	mol%

In the first approach (Case Study I), the recovery of H_2 from the abovementioned gas mixture is sought. Nowadays, this separation can be performed with state-of-the-art membrane materials. Principally, glassy polymers with their rigid structures lead to kinetically favorable H_2 permeability over other penetrants of higher kinetic diameter, i.e., for separation based on diffusivity selectivity. Consequently, a number of commercial polymers provide high selectivity towards H_2 with respect to N_2, CO and, to a lesser extent, CO_2 [9,27]. Recently, polymers of intrinsic microporosity (PIMs) have emerged as promising materials with extraordinary gas separation performance above Robeson's upper bound for many gas pairs. However, unlike other glassy polymers, PIMs present preferential CO_2 permeability [28] that would restrict the purity of the recovered H_2 in this application. Moreover, it is noteworthy that large-scale gas separations require highly productive membranes. This can be achieved processing membrane materials with asymmetric hollow fiber configuration that combines small dense layer thickness, preferably below 1 μm, and large surface area. Therefore, a polyimide is selected for this case study as reference membrane material that meets those features, i.e., polyimide membranes exhibit good separation performance for H_2 recovery and can be readily obtained as hollow fibers [29].

A more challenging strategy consisting on the simultaneous recovery of H_2 and CO from the flue gas of carbon black manufacturing is also considered here as Case Study II. Obtaining an enriched syngas stream would be the most beneficial approach in terms of increased resource use, as both H_2 and CO are recovered, as well as reduced environmental burdens, given that the CO_2 emissions related to the conventional thermal treatment of the flue gas are prevented. However, CO permeation through conventional polymeric membranes is severely hindered [26], except for some high-free volume polymers with low permeability selectivities. Yet a different emergent approach consisting on combining the potential as selective compounds of room-temperature ionic liquids (RTILs) with membrane technology can

Accepted manuscript

ACCEPTED MANUSCRIPT

effectively serve as a means to significantly improve the membrane performance for otherwise troublesome gas separations [30-32]. Specifically, facilitated-transport supported ionic liquid membranes (FT-SILMs) developed by our group have proved effective in separating H_2 and CO from N_2 owing to the combination of high H_2 permeability and enhanced CO/N_2 selectivity. In these membranes, CO permeability is improved by the selective and reversible complexation between CO and copper-based ionic liquids [33-35]. Although these types of membranes are under research and development, great effort has been made to obtain highly stable composite polymer/RTIL membranes and polymerized ionic liquid films [36]. Moreover, Fam et al. [37] have recently obtained the first composite polymer ionic liquid membranes in hollow fiber configuration with dense layer thicknesses between 1-2 μm, which are expected to be reduced for industrial applicability. Therefore, considering these promising results, hollow fiber FT-SILMs are selected as reference membranes for the purpose of obtaining enriched syngas from the flue gas stream.

Thus, based on experimental permeability data obtained in previous works [29,33,34], the membrane characteristics and separation performance of polyimide hollow fibers and FT-SILMs collected in Table 2 are considered for both case scenarios presented in this study.

Table 2. Reference membrane materials for each scenario.

Membrane features	Case Study I: H_2 recovery	Case Study II: Syngas recovery
Type	Polymeric	Composite polymer ionic liquid
Degree of development	Commercial	R&D
H_2 permeability (barrer[a])	30	50
Selectivity[b]:		
H_2/N_2	70.4	11.9
H_2/CO	38.5	4.6
H_2/CO_2	3.4	0.4
Dense layer thickness (μm)	0.35	0.90

[a] 1 barrer = 10^{-10} cm^3 (STP) cm cm^{-2} s^{-1} $cmHg^{-1}$. [b] Gas selectivity is reported as the ratio of pure gas permeabilities.

Process modeling

ACCEPTED MANUSCRIPT

As mentioned in the previous section, several studies aimed at designing optimal membrane-based separation networks are available in the literature. However, multistage and multistep combinations are rarely employed in commercial systems as they become uncompetitive compared with conventional gas separation technologies [38]. Therefore, as a first approximation, we consider the two-stage membrane system proposed by Baker et al. [38] whereby the feed gas is initially compressed and sent to the first separation stage in which the most permeable compounds are separated. Then, the permeate from the first stage is recompressed and sent to a second stage in which an enriched permeate is obtained. Alternatively, a two-step second stage can be used instead, where the retentate from the first unit is sent to a second unit without further recompression. In that case, the permeate from this second unit and the permeate from the first stage are mixed forming a recycle loop as illustrated in Figure 1. According to several authors [38,39], this design is more desirable and usual in industrial applications than complex three-stage systems. In fact, two-stage systems with recirculation are often found to be the optimal process layout in several of the previously mentioned studies [15-17,23].

In order to build the mathematical model of the hollow fiber membrane modules, the following assumptions are considered:

- Constant gas permeability regardless of pressure and composition.
- Ideal gas behavior and isothermal steady-state operation.
- Negligible pressure drop and concentration polarization effects.
- Plug flow pattern established in both feed and permeate side.
- Solution-diffusion model for gas transport through the membrane dense layer.

Accepted manuscript

ACCEPTED MANUSCRIPT

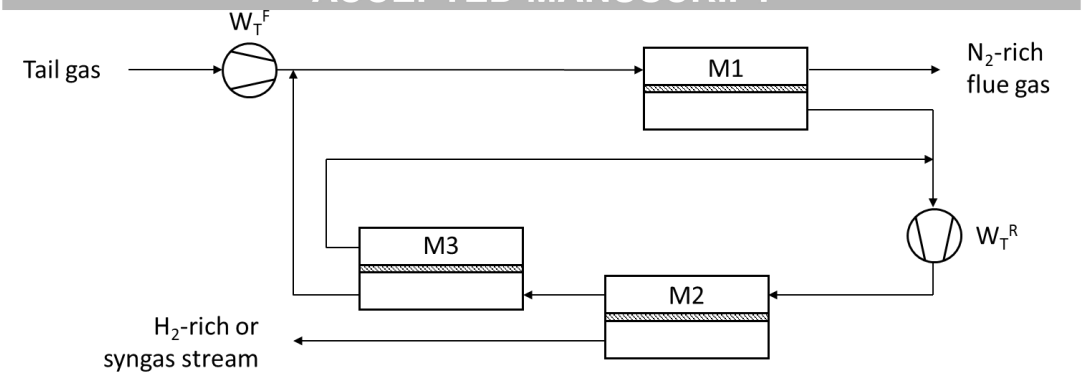

Figure 1. Two-stage membrane system, with an optional recycle loop (M3) around the second stage, proposed for the recovery of H_2 or syngas from dry tail gas.

A schematic diagram of the gas separation through a hollow fiber membrane operating in co-current configuration is presented in Figure 2. According to the solution-diffusion model, the mas transport flux of the components through the membrane, J_i, is given by:

$$J_i(z) = \frac{\mathrm{P}_i}{\delta} \cdot \left(p_i^F(z) - p_i^P(z) \right), \quad \forall i; \forall z \tag{1}$$

where P_i is the gas permeability of component i, δ is the dense layer thickness and p_i^F and p_i^P are the component partial pressures in the feed and permeate sides, respectively. Therefore, the differential mass balances around each component for a fiber slice of length dz are derived as follows:

$$dF_i^F(z) = -J_i(z) \cdot dA, \quad \forall i; \forall z \tag{2}$$

$$dF_i^P(z) = J_i(z) \cdot dA, \quad \forall i; \forall z \tag{3}$$

where F_i is the molar flowrate of component i and dA is the lateral area of the fiber slice. The following dimensionless variables and aggregate parameters are defined:

$$\bar{z} = \frac{z}{L} \tag{4}$$

Accepted manuscript

ACCEPTED MANUSCRIPT

$$\gamma = \frac{p^P}{p^F} \tag{5}$$

$$\overline{F_i}(z) = \frac{F_i(z)}{F^F_{T,z=0}}, \quad \forall i; \forall z \tag{6}$$

$$\Theta_i = \frac{A \cdot \mathrm{P}_i \cdot p^F}{\delta \cdot F^F_{T,z=0}}, \quad \forall i \tag{7}$$

$$x_i(z) = \frac{F_i^F(z)}{\sum F_i^F(z)}, \quad \forall i; \forall z \tag{8}$$

$$y_i(z) = \frac{F_i^P(z)}{\sum F_i^P(z)}, \quad \forall i; \forall z \tag{9}$$

which represent the molar fractions in the feed ($0 < x < 1$) and permeate ($0 < y < 1$) sides, the dimensionless axial length ($0 < \bar{z} < 1$), the pressure ratio between the permeate and feed sides ($0 < \gamma < 1$) , the dimensionless molar flowrates ($0 < \overline{F_i} < 1$) and the parameter Θ that groups together operating variables and design parameters; also, A and L represent the module area and fiber length, respectively.

Finally, combining Eqs. (1)-(9) yields the ordinary differential equations (ODEs) governing the mass transport through the hollow fiber membrane module in the feed and permeate sides:

$$\frac{d\overline{F_i^F}}{d\bar{z}} = -\Theta_i \cdot (x_i - \gamma y_i), \quad \forall i \tag{10}$$

$$\frac{d\overline{F_i^P}}{d\bar{z}} = \Theta_i \cdot (x_i - \gamma y_i), \quad \forall i \tag{11}$$

Accepted manuscript

ACCEPTED MANUSCRIPT

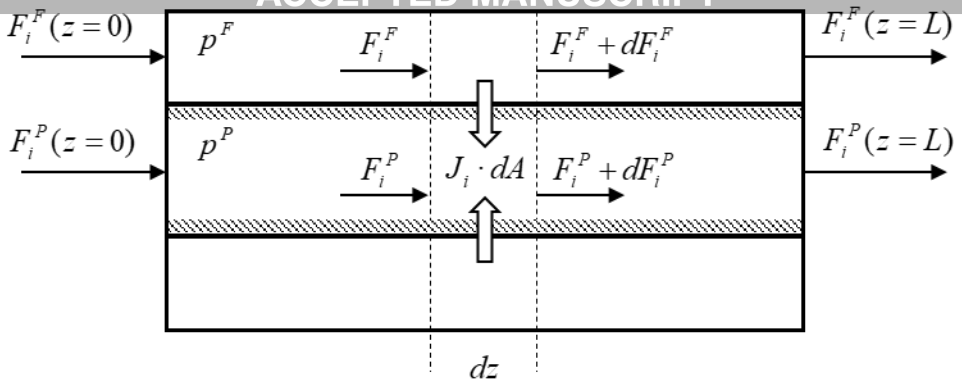

Figure 2. Schematic representation of a hollow fiber membrane stage with co-current feed (shell side) and permeate flows (lumen side).

The two ODEs given by Eqs. (10) and (11) can be solved when the boundary conditions at $\bar{z} = 0$ are given:

$$\left.\overline{F_i^F}\right|_{\bar{z}=0} = 1, \quad \forall i \tag{12}$$

$$\left.\overline{F_i^P}\right|_{\bar{z}=0} = 0, \quad \forall i \tag{13}$$

Finally, these ODEs are parametrized, considering implicit Runge-Kutta methods based on collocation, as Lagrange-form polynomials on finite elements over $\bar{z} \in [0,1]$ [40]:

$$\zeta_K(\bar{z}) = \sum_{j=0}^{K} \phi_j(\bar{z}) \cdot \zeta_{i,j} \,, \tag{14}$$

with $\phi_j(\bar{z}) = \prod_{\substack{k=0 \\ k \neq j}}^{K} \frac{(\bar{z} - \overline{z_{i,k}})}{(\overline{z_{i,j}} - \overline{z_{i,k}})}$

where i and k represent the number of finite elements and internal collocation points, respectively. Here, 100 finite elements are used for the fiber length, and 3 collocation points are used in each element.

Regarding the compressors, single-stage isothermal compression is usually considered to obtain a preliminary estimation of the compressor size. However, a more realistic approach

Accepted manuscript

ACCEPTED MANUSCRIPT

consists on considering that the feed and recycle compression are performed by isentropic staged compressors with equal compression ratios and then correcting the results by taking into account the isentropic compressor efficiency.

Economics

In this study, the membrane-based separation processes are optimized by determining the minimum net present value cost, NPV, to obtain a product stream that meets certain process specifications. The elements considered to calculate the NPV cost are the membrane modules and compressors, which are the main ancillary equipment related to membrane gas separations. Therefore, the NPV accounts for the capital costs, $CAPEX$, of the compressors and membrane modules as well as the operating costs, $OPEX$, due to electrical energy consumption and membrane replacement. Eventually, the capital and operating costs are related considering the time value of money [41]:

$$NPV = CAPEX + OPEX \cdot \left(1-\left(1+r\right)^{-T}\right)/r \qquad (15)$$

where r and T are the investment rate and period of time, respectively. The detailed equations used to assess the process economics are outlined in Appendix A and the main parameters listed in Table 3.

Table 3. Parameters used for cost estimation.

Parameter	Notation	Value	Unit
Compressor			
Compression stages	N_{st}	3 (p^F < 20.8 bar) 4 (p^F > 20.8 bar)	
Cost function exponent[a]	α	0.77	
Electricity price[b]	EP	0.15	\$/kWh
Isentropic efficiency	η_C	0.7	
Material and pressure factor[a]	MPF	1	
Maximum compression ratio	$CR_{\max}$	2.75	
Module factor[a]	MF	3.11	
Ratio of heat capacities	γ	1.4	
Reference cost[a]	C_0	23,000	\$
Reference size[a]	S_0	74.57	kW

ACCEPTED MANUSCRIPT

Update factor[c]	UF	4.71	
Membrane			
Membrane module cost	MC	50	$/m^2
Membrane replacement factor	MR	0.5	$/m^2/y
Project			
Annual operation	OF	8000	h/y
Investment rate	r	10	%
Period	T	15	y

[a] Based on Guthrie's cost estimation method [41]. [b] Based on average price for non-household consumers in the Euro area during the first half of 2017 [42]. [c] Calculated considering the chemical engineering plant cost index (CEPCI) for 2016.

Process optimization

The above set of equations was implemented in the General Algebraic Modeling System (GAMS v24.8) and the optimization problem mathematically formulated as:

$$\begin{aligned} \min_{x} \quad & NPV(x) \\ s.t. \quad & h_m(x) = 0, \quad \forall m \\ & g_n(x) \geq 0, \quad \forall n \\ & L \leq x \leq U \end{aligned} \tag{16}$$

where x is the vector of optimization variables, $h_m(x)$ are the model equations (8)-(14) and those included in Appendix A, $g_n(x)$ are the set of constraints described below and L and U are the vector of lower and upper bounds of the variables.

In this way the proposed model simultaneously optimized the operating conditions (feed pressure, composition and flowrate of all process streams), the membrane area in each stage as well as the power requirements to obtain the minimum net present value cost, given by Eq. (15), for each scenario. Process constraints, $g(x) \geq 0$, included in the optimization problem referred to the minimum H_2 recovery and purity of the product stream permeating from the second membrane module, which are given by: i) target H_2 recovery from the flue gas ($R_{H_2} \geq R_{H_2,\min}$), and ii) either H_2 purity in Case Study I ($P_I \geq P_{I,\min}$) or H_2+CO purity in Case Study II ($P_{II} \geq P_{II,\min}$). Moreover, a maximum compression ratio per stage was stablished (

Accepted manuscript

ACCEPTED MANUSCRIPT

$CR_{\max} \geq CR$). The design problem was formulated as a nonlinear programming (NLP) problem and solved using the local search optimization algorithm CONOPT. The execution time required to solve these NLP problems, which involved 12,314 variables and 12,316 constraints, was less than 0.2 s.

Results and discussion

In this section, we present the main results obtained after solving the optimization problem, given in Eq. (16), for the Case Study I and II subject to different H_2 recovery and product stream purity constraints. First, the general trends are analyzed separately for each recovery scenario and eventually, a comparison is performed between both case studies.

Case Study I

Regarding the recovery of H_2 from the flue gas stream considered in Case Study I, Fig. 3 presents the optimal values of the main process variables, i.e., feed side pressure, total compression duty, total membrane area and specific production costs, as well as the value of the objective function that is minimized for several H_2 recovery and product purity targets ranging from 70 to 90% and 86 to 96%, respectively, for the treatment of 100 kmol/h of flue gas with the specifications collected in Table 1. In these plots, each data series represents the set of optimal solutions obtained for the same product purity value as a function of the H_2 recovery target. Results indicate that the pressure to which the flue gas is compressed prior to each membrane separation stage is one of the main process variables that significantly affects the size of compressor stages as well as the required membrane area. As can be seen in Fig. 3a, the feed side gas pressure exponentially increases as the required H_2 recovery and product purity constraints become more demanding. Also, very high product purities can only be obtained at the expense of very high pressures and low recoveries, e.g., for the 96% H_2 purity

Accepted manuscript

ACCEPTED MANUSCRIPT

series a maximum of 77% H_2 recovery can be attained with four compression stages. However, it should be noted that the allowable maximum differential pressure of membrane-based gas separation processes will be limited by the mechanical resistance of the membrane material, which most likely will not surpass 20 bar [43]. Moreover, common feed to permeate pressure ratios in industrial gas separation processes are below 20, and typically in the range 5-15, in order to avoid the large expenses related to power usage and compressors capital costs [44]. Hence, the space of physically achievable H_2 recovery and purity targets for Case Study I is given in Fig. 3 by the optimization results represented by filled symbols, for which the optimal feed pressure is kept below a reasonable value of 15 bar.

Increasing the feed side gas pressure results in an increase of both the driving force, given that the permeate pressure is maintained at atmospheric pressure, and the power requirements, as shown in Fig. 3b. Consequently, the operating expenses related to the electricity consumption and the investment costs associated to the compressors size and number of compression stages also increase. It should be noted that the optimal total compression duty plotted in Fig. 3b exhibits a trend shift after a certain H_2 recovery target value that is attributed to the need of an additional compression stage. Hence, although gas pressure in the feed side is increased, the compression ratio is reduced with an additional stage and therefore, the required total compression work is similar. On the contrary, the required total membrane area and the related investment and replacement costs decrease as a consequence of the increase of the driving force as shown in Fig. 3c.

In summary, the optimization results plotted in Fig. 3d show the estimated specific production costs of the H_2-rich permeate product that is obtained with the proposed membrane material and process configuration at the minimum net present value cost (Fig. 3e) depending on the final purity and recovery values under consideration. As expected, the more demanding the recovery and purity constraints, the higher the specific production costs. For feed pressures below 15 bar and H_2 recoveries of 70%, these costs range between 0.12 and 0.15 \$/m^3 STP for

Accepted manuscript

ACCEPTED MANUSCRIPT

product purities between 86 and 92%, respectively. In all cases, the main impurity that appears in the permeate product stream is CO_2 due to the relatively low H_2/CO_2 selectivity of the polyimide membrane under consideration. Moreover, it is worth noticing that the specific production costs and the net present value cost exhibit a similar fashion, although the former has a less pronounced slope. This is reasonable as for this system the process throughput linearly increases with more demanding H_2 recoveries, hence the specific costs remain fairly constant over a wide range of H_2 recoveries.

Accepted manuscript

ACCEPTED MANUSCRIPT

(a)

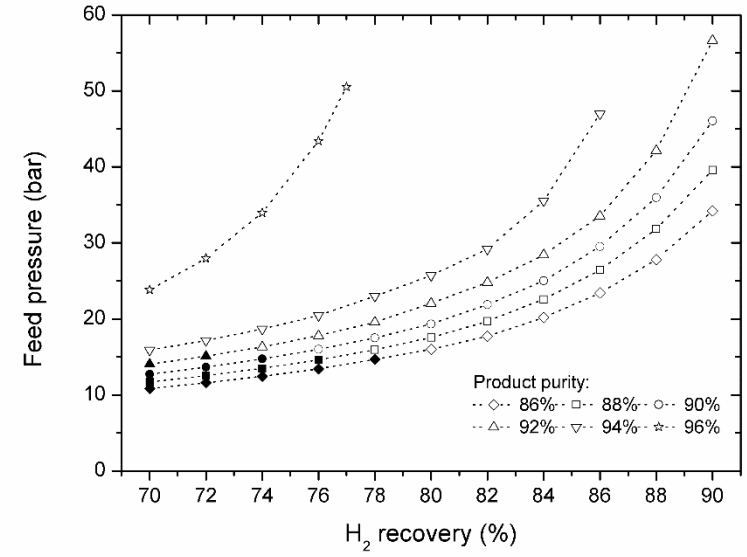

(b)

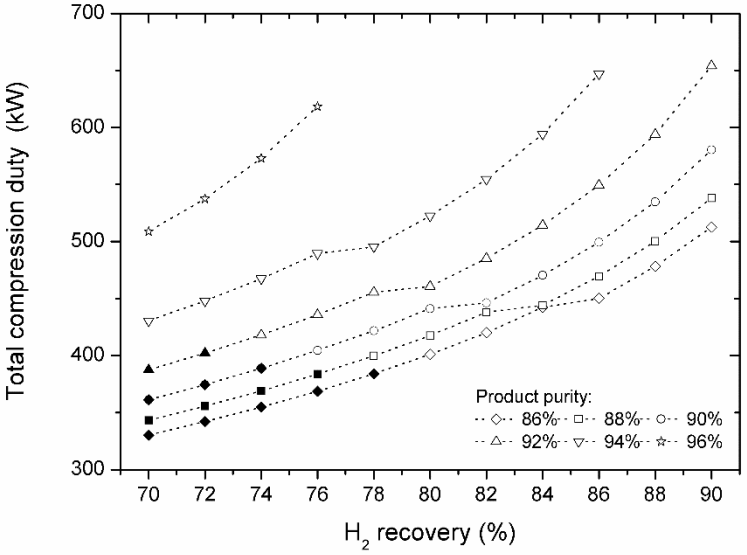

(c)

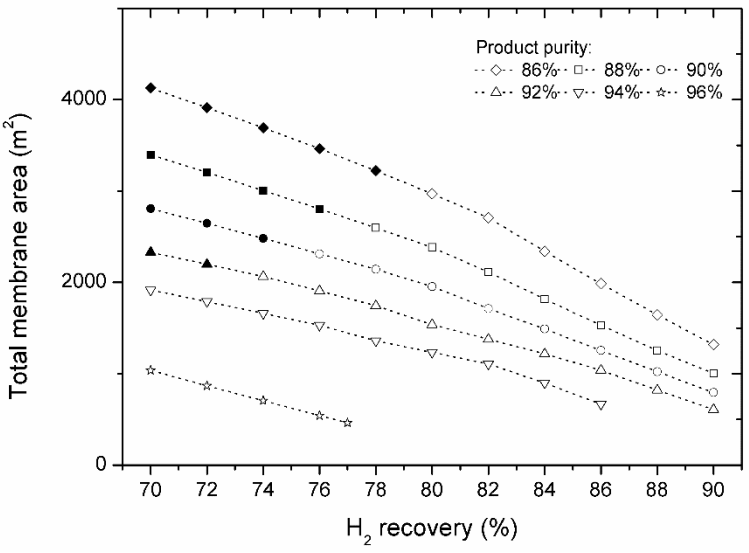

ACCEPTED MANUSCRIPT

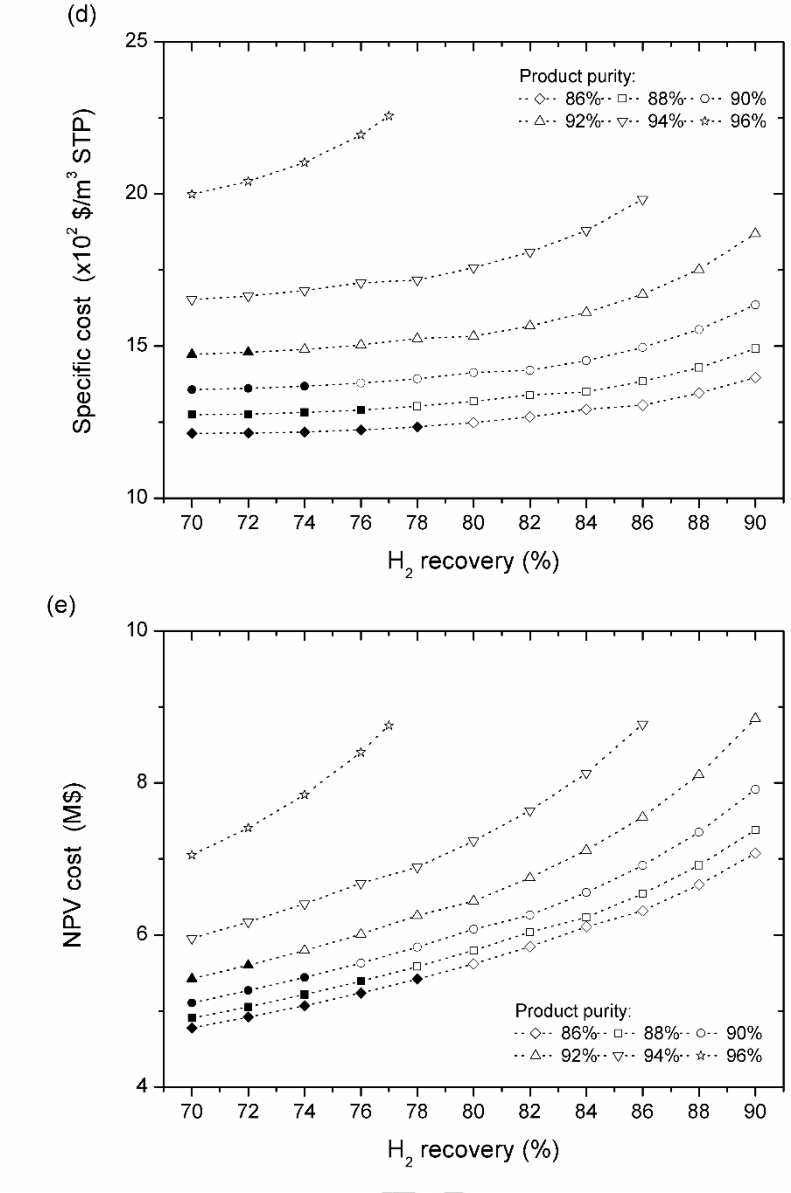

Figure 3. Optimal operating variables (Case Study I) as a function of H_2 recovery, ranging between 70 and 90%, and several H_2 purities of the product stream. (a) Feed pressure, (b) total compression duty, (c) total membrane area, (d) specific production cost and (e) minimum net present value cost. Filled symbols represent the feasibility region given by optimal feed pressures below 15 bar. Dotted lines are included to guide reader's eye.

An example of the optimal process design that minimized the specific production costs to obtain a H_2-rich stream (86% purity) and recover 78% of the initial flue gas H_2 content is illustrated in Fig. 4. In this process, the feed is compressed to 14.7 bar and only one step is

ACCEPTED MANUSCRIPT

required in the second membrane stage. It is worth noticing that the compression duty and membrane area needed in the enrichment section are 4- and 10-fold lower than in the first stage, respectively, given that the gas flowrate to be treated is much smaller. Consequently, the costs involved in this recycle loop does not significantly increase the overall expenses. Moreover, as previously explained, CO_2 represents the main impurity in the H_2-rich product stream (12.1 mol%) and just a residual amount of CO and N_2 is obtained (1.9 mol%).

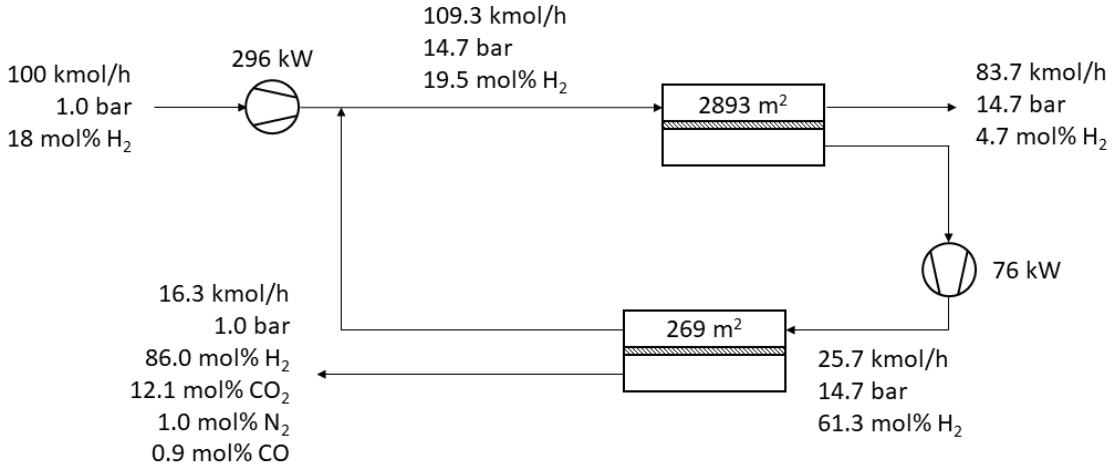

Figure 4. Optimal two-stage process design to achieve 78% H_2 recovery and obtain a H_2-rich permeate product stream (86% H_2 purity) in the Case Study I. Minimum net present value cost and specific production cost for this process layout are \$5.4 million, and 0.12 \$/m^3 STP, respectively.

Case Study II

The process optimization for obtaining syngas from the flue gas (Cases Study II) is assessed following the same previous methodology for several H_2 recovery and H_2+CO purity targets ranging from 76 to 96% and 68 to 78%, respectively. As shown in Fig. 5, the results found for the optimal values of the main process variables exhibit similar, yet less marked, trends than the previous case study. That is, the required feed pressure (Fig. 5a) and total compression duty (Fig. 5b) increase as the H_2 recovery and H_2+CO purity targets become more demanding. Again, if a pressure limit of 15 bar is assumed to define the region of physically achievable

Accepted ma

ACCEPTED MANUSCRIPT

results in Fig. 5, it becomes clear that this approach allows working in a wider range of H_2 recoveries and syngas purities than before. The total membrane area, shown in Fig. 5c, also decreases with higher differential pressure gradients and H_2 recoveries. However, as the H_2+CO purity is increased, the required area of the first and second separation steps decrease and that of the third step becomes significantly important. Consequently, the relative reduction of total membrane area becomes less significant as the H_2+CO purity and feed pressure increase.

In addition, it is interesting to determine the amount of CO that can be recovered together with H_2 and the characteristics of the syngas-rich permeate product. In this sense, Fig. 5d and Fig. 5e present the final CO recovery and syngas ratio (H_2:CO) that could be obtained with the novel ionic liquid-based membranes. As can be seen, the CO recovery increases with increasing H_2 recovery whereas the H_2:CO ratio slightly decreases. However, these variables exhibit opposite trends with respect to the H_2+CO purity in the permeate product, i.e., CO recovery decreases and H_2:CO ratio increases because of the increase of H_2+CO purity. For feed pressures below 15 bar, achievable CO recoveries and H_2:CO ratios range between 16-48% and 2-5.5, respectively. With respect to the main impurities of the syngas product, significant amounts of both N_2 (6-22 mol%) and CO_2 (10-16 mol%) are found in the permeate stream. Although the presence of a certain amount of inert gases is acceptable for some applications, e.g., Fischer-Tropsch reactions, for other synthesis gas reactions the inert gas components have to be very low. However, given that these ionic liquid-based membranes are still in an incipient development stage, their gas separation performance is likely to improve soon. Particularly, more N_2-rejective materials are sought to yield a syngas product with residual N_2 content. Finally, Fig. 5f shows the estimated specific production costs of the syngas product obtained at the minimum net present value cost (Fig. 5g) as a function of the H_2 recovery and H_2+CO purity targets. For H_2 recoveries of 86% and H_2+CO purities between 68 and 78%, these costs range between 0.07 and 0.12 \$/m^3 STP, respectively.

Accepted manuscript

ACCEPTED MANUSCRIPT

A comparison between the optimization results obtained for the recovery scenarios proposed in Case Study I and II indicates that it would be possible to obtain a syngas-rich product stream achieving much higher H_2 and CO recoveries than in Case Study I. Considering the feed pressure threshold of 15 bar, a maximum of 86% H_2 recovery was achieved in Case Study I; whereas, up to 90% and 43% of the initial H_2 and CO, respectively, can be recovered at pressures below that limit according to the results obtained in Case Study II. Consequently, the recovery of value-added compounds is intensified in the case of obtaining syngas-rich instead of H_2-rich permeates, yet at the expense of obtaining less pure product streams. An example of such syngas recovery from the process flue gas is illustrated in Fig. 6, in which 80% and 27.2% of the initial H_2 and CO content are recovered, respectively. In this example, the H_2+CO purity in the permeate product stream is 74% and the presence of CO_2 and N_2 is still significant, thus indicating that more selective membranes would be required to further minimize the inert gas components as previously stated. An overview of the optimal process designs obtained for Case Study I and II also reveals that the production of syngas from the tail gas under analysis by means of state-of-the-art membranes would require larger membrane areas and lower feed pressures than obtaining a H_2-rich product. However, the simultaneous recovery of H_2 and CO significantly increases the production rates and therefore, the specific production costs are much lower than in Case Study I, although the gas separation process is performed at the expense of similar compression duties.

Accepted manuscript

(a)

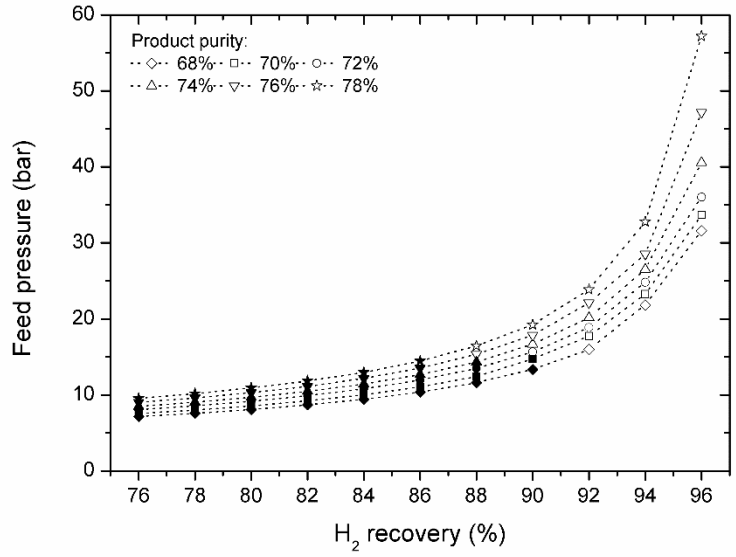
Product purity:
68% 70% 72%
74% 76% 78%
Feed pressure (bar)
H2 recovery (%)

(b)

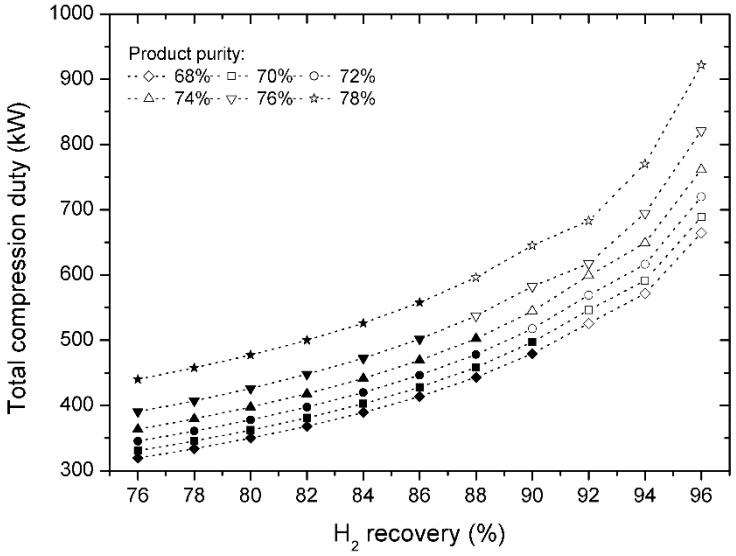
Product purity:
68% 70% 72%
74% 76% 78%
Total compression duty (kW)
H2 recovery (%)

(c)

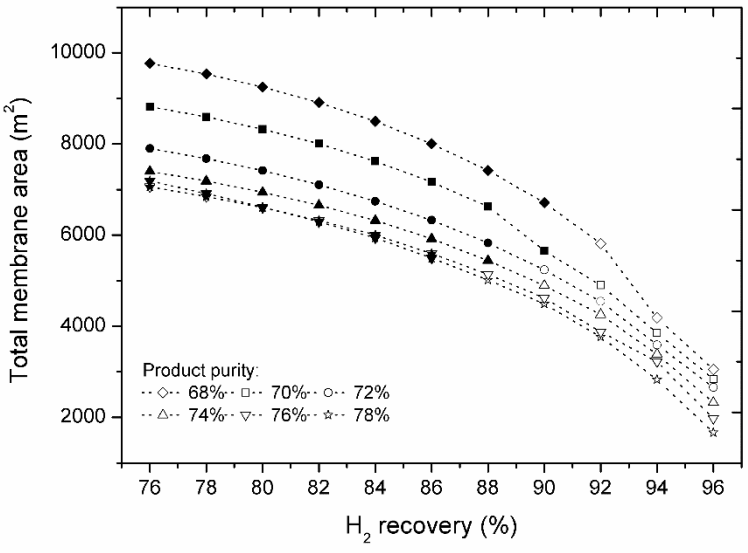
Product purity:
68% 70% 72%
74% 76% 78%
Total membrane area (m2)
H2 recovery (%)

(d)

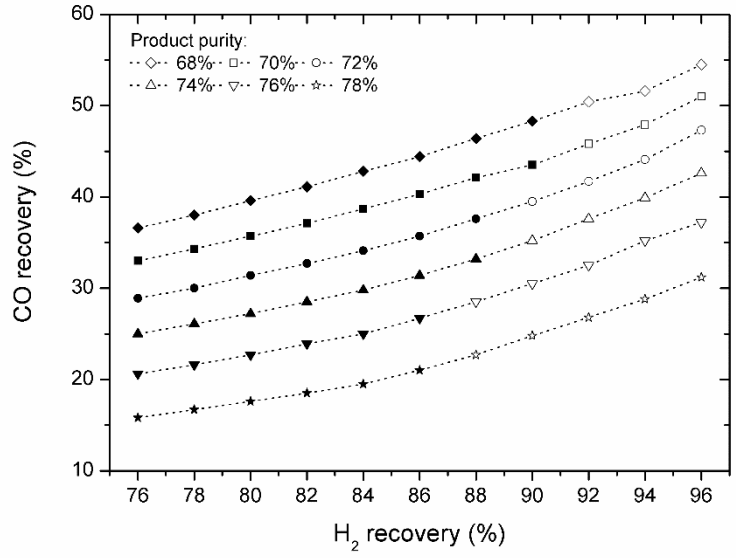
Product purity:
68% 70% 72%
74% 76% 78%
CO recovery (%)
60
50
40
30
20
10
76 78 80 82 84 86 88 90 92 94 96
H2 recovery (%)

(e)

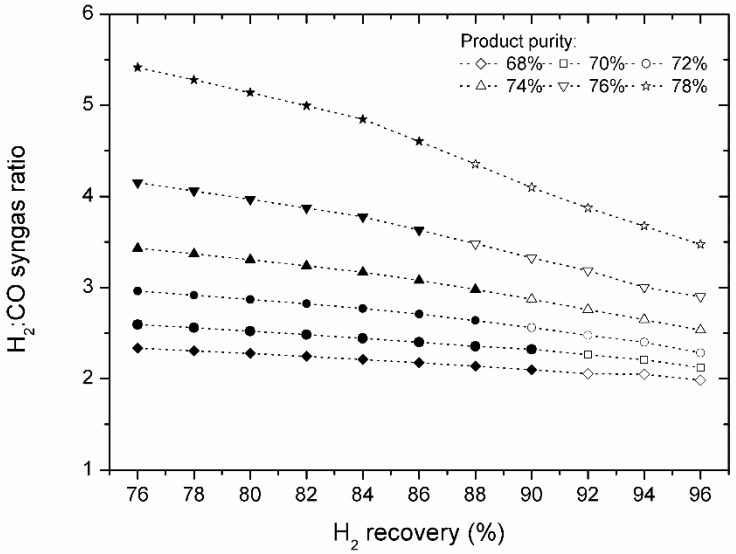
Product purity:
68% 70% 72%
74% 76% 78%
H2:CO syngas ratio
6
5
4
3
2
1
76 78 80 82 84 86 88 90 92 94 96
H2 recovery (%)

(f)

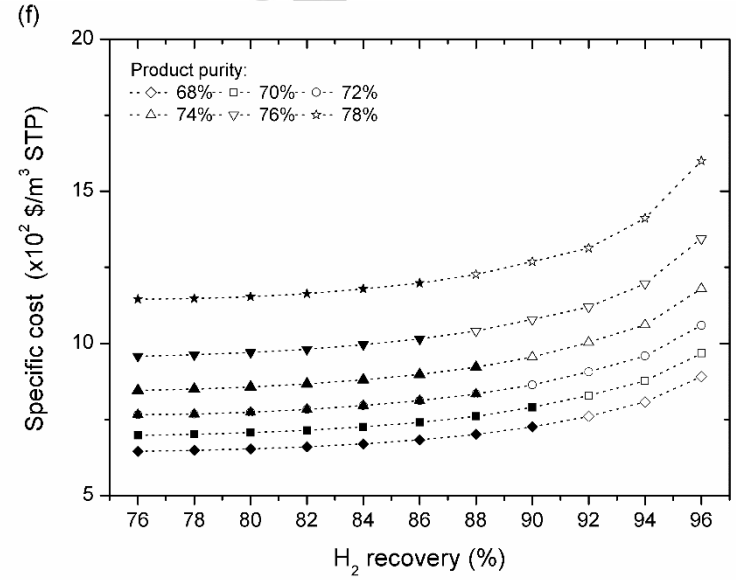
Product purity:
68% 70% 72%
74% 76% 78%
Specific cost (x10² $/m³ STP)
20
15
10
5
76 78 80 82 84 86 88 90 92 94 96
H2 recovery (%)

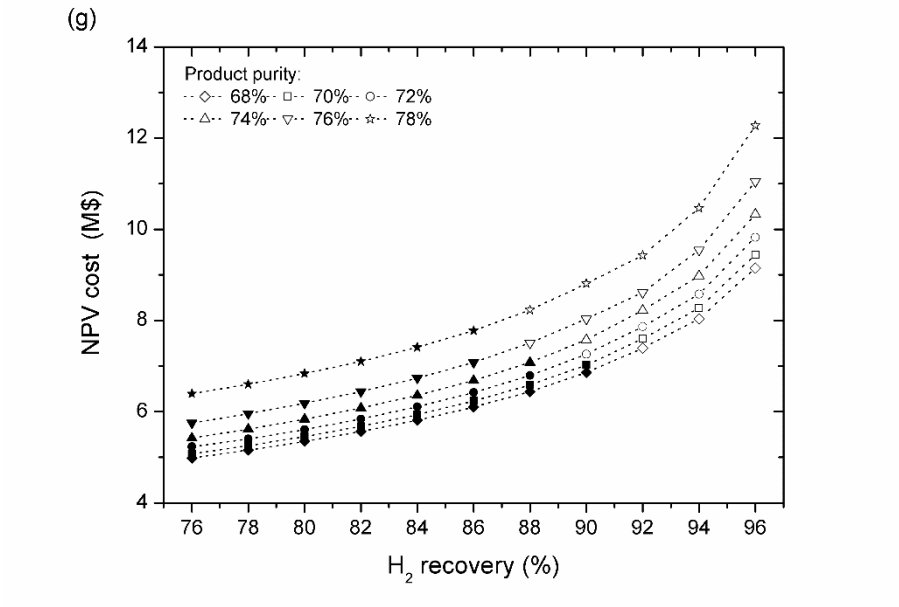

Figure 5. Optimal operating variables (Case Study II) as a function of H_2 recovery, ranging between 76 and 96%, and several H_2+CO purities of the product stream. (a) Feed pressure, (b) total compression duty, (c) total membrane area, (d) CO recovery, (e) product syngas ratio (H_2:CO), (f) specific production cost and (g) minimum net present value cost. Filled symbols represent the feasibility region given by optimal feed pressures below 15 bar. Dotted lines are included to guide reader's eye.

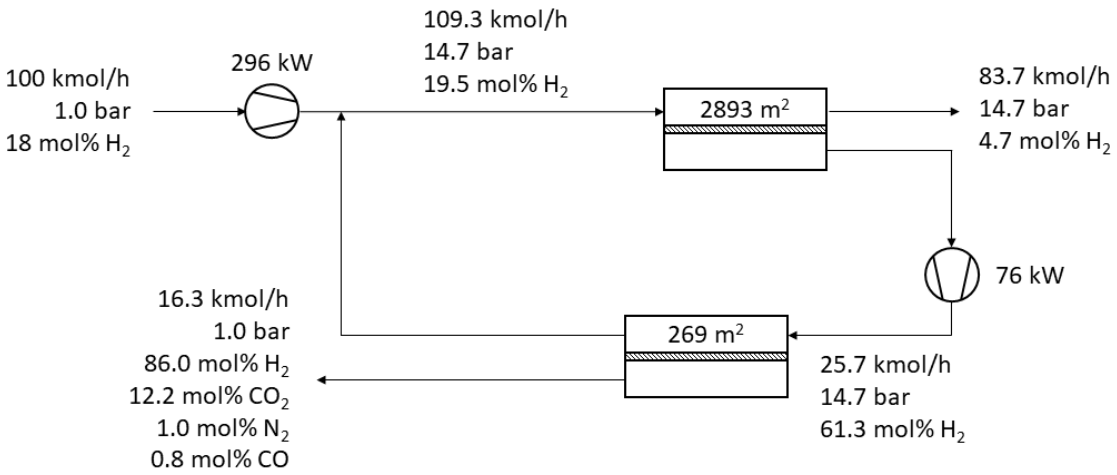

Figure 6. Optimal two-and-one-half stage membrane system to achieve 80% H_2 recovery and obtain a syngas-rich permeate product stream (74% H_2+CO purity) in the Case Study II.

ACCEPTED MANUSCRIPT

Minimum net present value cost and specific production cost for this process layout are \$5.8 million, and 0.09 \$/m^3 STP, respectively.

Sensitivity analysis

In this section, a comprehensive sensitivity analysis is performed to investigate the influence on the optimal process design of several key parameters used for cost estimation and membrane features, namely, membrane module cost per unit area, electricity price, dense layer thickness, H_2 permeability (maintaining the gas pair selectivities unchanged) and H_2 selectivity with respect to the main component of the flue gas (N_2). To that end, the examples shown in Fig. 4 (Case Study I: 78% H_2 recovery and 86% H_2 purity) and Fig. 6 (Case Study II: 80% H_2 recovery and 74% H_2+CO purity) are selected as the base cases and two different scenarios are proposed for each of them in order to analyze the sensitivity of the optimal designs to changes in the abovementioned variables. That is, the best and worst scenarios are defined by giving new values to the variables selected to perform the analysis, as shown in Table 4. Then, the sensitivity analysis is performed by changing the value of one variable while maintaining others in their respective base case values. In this way, the influence of these variables on the optimal design for each case study is assessed independently.

Table 4. Parameters and membrane features considered in the sensitivity analysis.

Variable	Base case	Best scenario	Worst scenario
Membrane module cost (\$/m^2)	50	25	250
Electricity price (\$/kWh)	0.15	0.08	0.19
Dense layer thickness (μm):			
Case Study I	0.35	0.2	1
Case Study II	0.9	0.6	1.5
H_2 permeability (barrer):			
Case Study I	30	90	25
Case Study II	50	80	30
H_2/N_2 selectivity:			
Case Study I	70.4	90	25
Case Study II	11.9	25	7

Accepted manuscript

ACCEPTED MANUSCRIPT

The influence of these variables on the minimum net present value cost is shown in Figure 7 as the relative change of the objective function with respect to the base case value. As can be seen, the costs associated to the membrane module and electricity price have a significant influence on the optimal solution of both case studies. For instance, the minimum net present value cost increases around 10% (Case Study I) and 17% (Case study II) when the membrane cost is 250 \$/m^2 instead of the base case value (50 \$/m^2). Nevertheless, recent studies only contemplate membrane costs ranging between the base case value selected in this work [14,16,17] and 100 \$/m^2 [15,19]. Regarding the electricity price, the optimal net present value cost increases ~17% and decreases ~30% for the worst and best scenario, respectively, which account for country differences in electricity price within the Euro area [42]. On the other hand, the optimal process design for the example of Case Study II is considerably more sensitive to the membrane features assessed. In this sense, results shown in Fig. 7b indicate that the minimum net present value cost can be significantly reduced if novel composite membranes with improved H_2-selectivity properties are developed. In contrast, the H_2/N_2 selectivity of polymer membranes in the best scenario of Case Study I is close to the current upper bound [11]. Thus, it is likely that further enhancements for pure H_2 recovery come at the hands of process design rather than improving the membrane separation performance.

pted manuscript

(a)

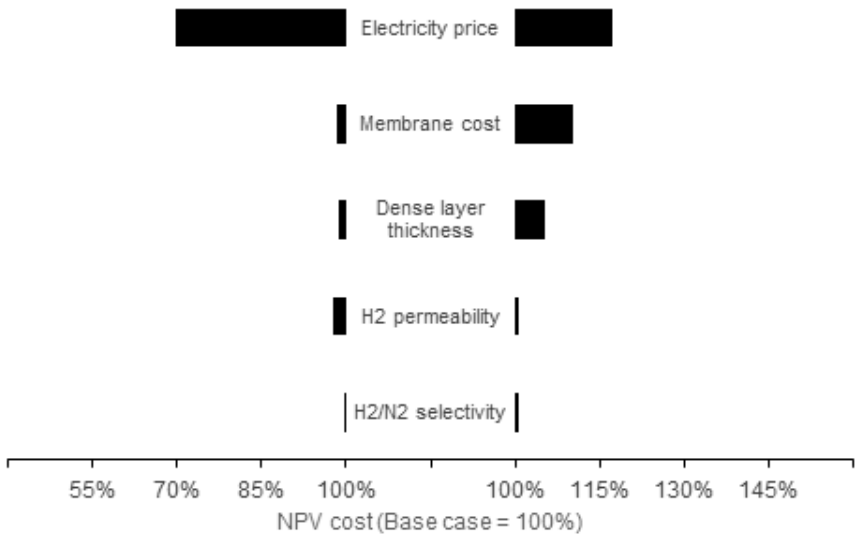

ACCEPTED MANUSCRIPT

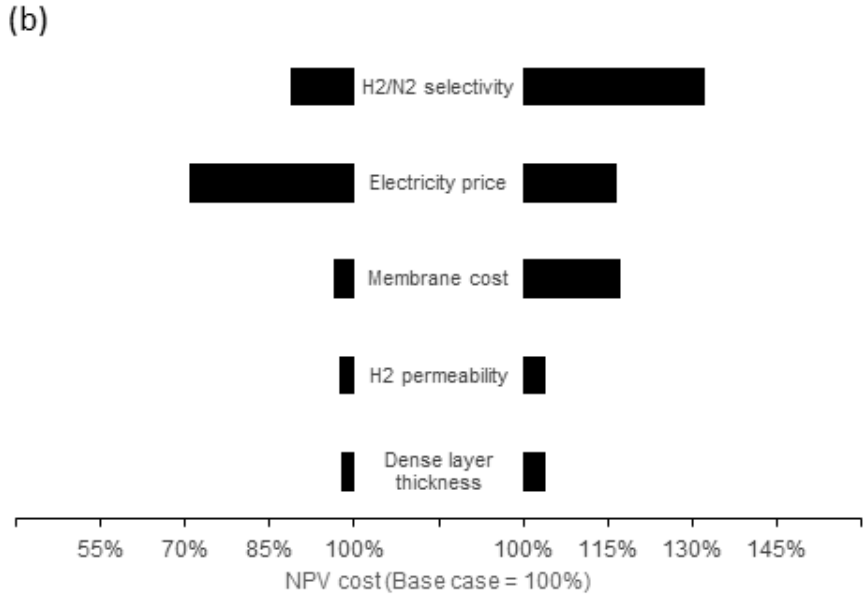

Figure 7. Influence of cost estimation parameters and membrane features on the optimal process designs. Results are shown as the relative change of minimum net present value cost with respect to the base case considering the best scenario (left-side bars) and worst scenario (right-side bars). (a) Case Study I (78% H_2 recovery and 86% H_2 purity) and (b) Case Study II (80% H_2 recovery and 74% H_2+CO purity).

Accepted manuscript

Conclusions

In this work, an optimization model is proposed to assess the viability of using membrane technology for recovering value-added compounds from post-combustion gas generated in carbon manufacturing process. Particularly, we show how the use of modeling and optimization tools can help to discriminate between two different approaches, the recovery of either H_2 or syngas, highlighting the influence of membrane materials on the optimal process design that minimizes the net present value cost for several scenarios.

Despite the significant content of unvalued N_2 in the tail gas, the results presented show that a simple two-stage membrane process can be applied to the recovery of significant amounts of H_2 employing state-of-the-art membrane materials available on a commercial scale.

ACCEPTED MANUSCRIPT

Furthermore, the use of novel polymer ionic liquid composite membranes seems very promising for the alternative approach aimed at obtaining a syngas-rich product at the expense of lower power requirements and specific production costs. In this way, not only the recovery of value-added compounds is intensified, but also CO_2 emissions generated in the conventional thermal treatment of the tail gas can be reduced. Hence, this approach leads to additional environmental and economic advantages considering the current Emissions Trading System within the European framework. However, the technical viability of this recovery strategy requires that research efforts are placed on the development of composite polymer/ionic liquid hollow fiber membranes with enhanced mechanical properties and improved separation performance. In particular, the availability of composite membranes with ultrathin selective layers that can provide superior N_2-rejective properties seems crucial in order to further increase the H_2 and CO recoveries as well as the purity of the syngas permeate product stream.

Accepted manuscript

Acknowledgements

Financial support from the Spanish Ministry of Economy and Competitiveness (CTQ2015-66078) is gratefully acknowledged.

Appendix A

The capital expenses are calculated considering the investment costs of membranes (CC_M) and feed and recycle staged compressors (CC_C^F and CC_C^R):

$$CAPEX = CC_M + CC_C^F + CC_C^R \quad \text{(A.1)}$$

ACCEPTED MANUSCRIPT

The membrane costs are given by:

$$CC_M = MC \cdot A_T \quad \text{(A.2)}$$

where MC is the membrane module cost per unit area and A_T is the total membrane area.

The following equations are used to estimate the base (BC_C) and capital costs (CC_C) of the feed and recycle compressors from their individual capacities [41]:

$$BC_C = C_0 \cdot \left(\frac{W_T}{N_{st} \cdot S_0} \right)^{\alpha} \quad \text{(A.3)}$$

$$CC_C = N_{st} \cdot UF \cdot BC_C \cdot (MPF + MF - 1) \quad \text{(A.4)}$$

where C_0 is the compressor reference cost, W_T is the total feed or recycle compression duty, N_{st} is an integer number of compression stages, S_0 is the compressor reference size, α is the cost function exponent, UF is the update factor, MPF is the material and pressure factor and MF is the module factor.

The number of compression stages, the compression ratio (CR), the outlet pressure (p^F) and the total compression duty (W_T) are related as follows [41]:

$$\left(\frac{p^F}{p_0} \right)^{1/Nst} = CR \quad \text{(A.5)}$$

$$W_T = \frac{F}{\eta_C} \cdot N_{st} \cdot \left(\frac{\gamma}{\gamma - 1} \right) \cdot R \cdot T_0 \cdot \left(\left(\frac{p^F}{p_0} \right)^{(\gamma-1)/(\gamma \cdot Nst)} - 1 \right) \quad \text{(A.6)}$$

where η_C is the isentropic compressor efficiency, γ is the ratio of heat capacities, R is the universal gas constant and T_0 is the inlet temperature.

Accepted manuscript

ACCEPTED MANUSCRIPT

The operating expenses due to electricity consumption of feed and recycle compressors and membrane replacement are given by:

$$OPEX = \left(W_T^F + W_T^R\right) \cdot OF \cdot EP + A_T \cdot MR \quad \text{(A.7)}$$

where OF is the annual operating factor, EP is the electricity price and MR is the membrane replacement factor.

The H_2 recovery obtained in the product stream (permeate from the second membrane module), R_{H_2}, is given by:

$$R_{H_2} = \frac{F_{H_2}^P\left(z = L\right)}{F_0 \cdot x_0^{H_2}} \quad \text{(A.8)}$$

And the product purity in each case study, P_I or P_{II}, is calculated as follows:

$$P_I = \frac{F_{H_2}^P\left(z = L\right)}{\sum_i F_i^P\left(z = L\right)} \quad \text{(A.9)}$$

$$P_{II} = \frac{F_{H_2}^P\left(z = L\right) + F_{CO}^P\left(z = L\right)}{\sum_i F_i^P\left(z = L\right)} \quad \text{(A.10)}$$

Accepted manuscript

References

[1] P. Ghisellini, C. Cialani, S. Ulgiati, A review on circular economy: the expected transition to a balanced interplay of environmental and economic systems, J. Clean. Prod. 114 (2016) 11-32.

[2] R. Remus, M.A. Aguado-Monsonet, S. Roudier, L.D. Sancho. Best Available Techniques (BAT) reference document for iron and steel production. European Commission, Institute for

ACCEPTED MANUSCRIPT

Prospective Technological Studies, Technologies for Sustainable Development, European IPPC Bureau, 2013, Sevilla – Spain.

[3] A.A. Ramírez-Santos, C. Castel, E. Favre, A review of gas separation technologies within emission reduction programs in the iron and steel sector: Current application and development perspectives, Sep. Purif. Technol. 194 (2018) 425-442.

[4] T. Abbasi, S.A. Abbasi, 'Renewable' hydrogen: Prospects and challenges, Renew. Sust. Energ. Rev. 15 (2011) 3034–3040.

[5] N. Armaroli, V. Balzani, The hydrogen issue, Chem. Sus. Chem. 4 (2011) 21-36.

[6] J.D. Perry, K. Nagai, W.J. Koros, Polymer membranes for hydrogen separations, MRS Bull. 31 (2006) 745-749.

[7] D.S. Sholl, R.P. Lively, Seven chemical separations to change the world, Nature 532 (2016) 435-437.

[8] P. Bernardo, E. Drioli, G. Golemne, Membrane gas separation: A review/state of the art, Ind. Eng. Chem. Res. 48 (2009) 4638-4663.

[9] L. Shao, B.T. Low, T.-S. Chung, A.R. Greenberg, Polymeric membranes for the hydrogen economy: Contemporary approaches and prospects for the future, J. Membr. Sci. 327 (2009) 18-31.

[10] R.W. Baker, B.T. Low, Gas separation membrane materials: a perspective, Macromolecules 47 (2014) 6999-7013.

[11] L.M. Robeson, The upper bound revisited, J. Membr. Sci. 320 (2008) 390-400.

[12] L. Zhao, E. Riensche, R. Menzer, L. Blum, D. Stolten, A parametric study of CO_2/N_2 gas separation membrane processes for post-combustion capture, J. Membr. Sci. 325 (2008) 284-294.

Accepted manuscript

ACCEPTED MANUSCRIPT

[13] M. Yuan, K. Narakornpijit, R. Haghpanah, J. Wilkox, Consideration of a nitrogen-selective membrane for postcombustión carbon capture through process modeling and optimization, J. Membr. Sci. 465 (2014) 177-184.

[14] A. Aliaga-Vicente, J.A. Caballero, M.J. Fernández-Torres. Synthesis and optimization of membrane cascade for gas separation via mixed-integer nonlinear programming, AIChE J. 63 (2017) 1989-2006.

[15] B. Ohs, J. Lohaus, M. Wessling, Optimization of membrane based nitrogen removal from natural gas, J. Membr. Sci. 498 (2016) 291-301.

[16] A.M. Arias, M.C. Mussati, P.L. Mores, N.J. Scenna, J.A. Caballero, S.F. Mussati, Optimization of multi-stage membrane systems for CO_2 capture from flue gas, Int. J. Greenh. Gas Con. 53 (2016) 371-390.

[17] M. Scholz, M. alders, T. Lohaus, M. Wessling, Structural optimization of membrane-based biogas upgrading process, J. Membr. Sci. 474 (2015) 1-10.

[18] R. Pathare, R. Agrawal, Design of membrane cascades for gas separation, J. Membr. Sci. 3646 (2010) 263-277.

[19] R.V.S. Uppaluri, R. Smith, P. Linke, A.C. Kokossis, On the simultaneous optimization of pressure and layout for gas permeation membrane systems, J. Membr. Sci. 280 (2006) 832-848.

[20] I.K. Kookos, A targeting approach to the synthesis of membrane networks for gas separations, J. Membr. Sci. 208 (2002) 193-202.

[21] R. Qi, M.A. Henson, Optimal design of spiral-wound membrane networks for gas separations, J. Membr. Sci. 148 (1998) 71-89.

Accepted manuscript

ACCEPTED MANUSCRIPT

[22] R. Qi, M.A. Henson, Membrane system design for multicomponent gas mixtures via mixed-integer nonlinear programming, Comput. Chem. Eng. 24 (2000) 2719-2737.

[23] P. Gabrielli, M. Gazzani, M. Mazzotti, On the optimal design of membrane-based gas separation processes, J. Membr. Sci. 526 (2017) 118-130.

[24] J. Marriott, E. Sorensen, The optimal design of membrane systems, Chem. Eng. Sci. 58 (2003) 4991-5004.

[25] Reference document on Best Available Techniques (BAT) for the manufacture of large volume inorganic chemicals – solids and others industry. European Commission, Institute for Prospective Technological Studies, Technologies for Sustainable Development, European IPPC Bureau, 2007, Sevilla – Spain.

[26] C.A. Scholes, S.E. Kentish, G.W. Stevens, Effects of minor components in carbon dioxide capture using polymeric gas separation membranes, Sep. Purif. Rev. 38 (2009) 1-44.

[27] O.C. David, D. Gorri, A. Urtiaga, I. Ortiz, Mixed gas separation study for the hydrogen recovery from $H_2/CO/N_2/CO_2$ post combustion mixtures using a Matrimid membrane, J. Membr. Sci. 378 (2011) 359-368.

[28] P.M. Budd, K.J. Msayib, C.E. Tattershall, B.S. Ghanem, K.J. Reynolds, N.B. McKeown, D. Fritsch, Gas separation membranes from polymers of intrinsic microporosity, J. Membr. Sci. 251 (2005) 263-269.

[29] O.C. David, D. Gorri, K. Nijmeijer, I. Ortiz, A. Urtiaga, Hydrogen separation from multicomponent gas mixtures containing CO, N2 and CO2 using Matrimid® asymmetric hollow fiber membranes, J. Membr. Sci. 419-420 (2012) 49-56.

[30] Z. Dai, R.D. Noble, D.L. Gin, X. Zhang, L. Deng, Combination of ionic liquids with membrane technology: a new approach for CO_2 separation, J. Membr. Sci. 497 (2016) 1–20.

Accepted manuscript

ACCEPTED MANUSCRIPT

[31] R. Zarca, A. Ortiz, D. Gorri, I. Ortiz, Generalized predictive modeling for facilitated transport membranes accounting for fixed and mobile carriers, J. Membr. Sci. 542 (2017) 168-176.

[32] A. Ortiz, M.L. Galán, D. Gorri, A.B. de Haan, I. Ortiz. Reactive ionic liquid media for the separation of propylene/propane gaseous mixtures. Ind. Eng. Chem. Res. 49 (2010) 7227-7233.

[33] G. Zarca, I. Ortiz, A. Urtiaga, Copper(I)-containing supported ionic liquid membranes for carbon monoxide/nitrogen separation, J. Membr. Sci. 438 (2013) 38–45.

[34] G. Zarca, I. Ortiz, A. Urtiaga, Facilitated-transport supported ionic liquid membranes for the simultaneous recovery of hydrogen and carbon monoxide from nitrogen-enriched gas mixtures, Chem. Eng. Res. Des. 92 (2014) 764–768.

[35] G. Zarca, I. Ortiz, A. Urtiaga, Novel solvents based on thiocyanate ionic liquids doped with copper(I) with enhanced equilibrium selectivity for carbon monoxide separation from light gases, Sep. Purif. Technol. 196 (2018) 47-56.

[36] G. Zarca, W.J. Horne, I. Ortiz, A. Urtiaga, J.E. Bara, Synthesis and gas separation properties of poly(ionic liquid)-ionic liquid composite membranes containing a copper salt, J. Membr. Sci. 515 (2016) 109-114.

[37] W. Fam, J. Mansouri, H. Li, V. Chen, Improving CO_2 separation performance of thin film composite hollow fiber with Pebax®1657/ionic liquid gel membranes, J. Membr. Sci. 537 (2017) 54-68.

[38] R.W. Baker, Gas separations, in: Membrane Technology and Applications, John Wiley & Sons, Chichester, 2012.

[39] E. Favre, Polymeric membranes for gas separation, in: E. Drioli, L. Giorno (Eds.), Comprehensive Membrane Science and Engineering, Elsevier, Oxford, 2010.

Accepted manuscript

ACCEPTED MANUSCRIPT

[40] L.T. Biegler (Ed.), Nonlinear Programming: Concepts, Algorithms, and Applications to Chemical Processes, Society for Industrial and Applied Mathematics, Philadelphia, 2010.

[41] L.T. Biegler, I.E: Grossmann, A.W. Westerberg (Eds.), Systematic Methods of Chemical Process Design, Prentice Hall PTR, New Jersey, 1997.

[42] Eurostat Statistics Explained, Electricity price statistics. http://ec.europa.eu/eurostat/statistics-explained/index.php/Electricity_price_statistics, 2017 (accessed December 2017).

[43] Y. Huang, T.C. Merkel, R.W. Baker, Pressure ratio and its impact on membrane gas separation processes, J. Membr. Sci. 463 (2014) 33-40.

[44] S. Sato, K. Nagai, Polymer membranes with hydrogen-selective and hydrogen-rejective properties. Membr. J. 30 (2005) 20-28.

Accepted manuscript

ACCEPTED MANUSCRIPT

Highlights

- Optimization model for membrane-based flue gas valorization.
- Optimal process design for several scenarios based on NPV cost minimization.
- State-of-the-art and prospective membrane materials assessed.
- Results highlight potential of polymer/ionic liquid membranes for syngas recovery.

Accepted manuscript